Elastic Solutions for Laterally Loaded Piles

William Higgins, S.M.ASCE[1]; Celio Vasquez[2]; Dipanjan Basu, M.ASCE[3]; and D. V. Griffiths, F.ASCE[4]

Abstract: Laterally loaded piles are analyzed using the Fourier FEM. The analysis is performed for piles embedded in single-layer elastic soil with constant and linearly varying modulus and in two-layer elastic soil with constant modulus within each layer. The pile responses were observed to be functions of the relative stiffness of pile and soil, and of the pile slenderness ratio. Based on the analysis, equations describing pile head deflection, rotation, and maximum bending moment are proposed for flexible long piles and stubby rigid piles. These design equations are developed after plotting the pile responses as functions of pile-soil stiffness ratio and pile slenderness ratio. These plots can also be used as design charts. Design examples illustrating the use of the analysis are provided. **DOI: 10.1061/(ASCE)GT.1943-5606.0000828.** © *2013 American Society of Civil Engineers.*

CE Database subject headings: Piles; Lateral loads; Finite element method; Elasticity; Design.

Author keywords: Pile; Lateral load; Finite element analysis; Elasticity; Design.

Introduction

Structures resting on piles are frequently subjected to horizontal forces from wind, traffic, and seismic activities. The horizontal forces acting on tall or heavy structures like high-rise buildings, bridge abutments, and earth-retaining structures are often of very large magnitude. Offshore structures like quays and harbors are also subjected to large lateral forces arising out of wind, waves, and ship berthing. The horizontal forces eventually get transmitted to the piles, which are analyzed considering a concentrated force and/or moment acting at the pile head. Even in structures where piles are used to resist vertical forces only, there may exist moments from load eccentricities caused by faulty construction. Consequently, proper analysis and design of piles subjected to lateral forces and moments is very important to ensure the stability and serviceability of various structures.

Numerous research studies, both theoretical and experimental, have been performed on laterally loaded piles for more than six decades. The early theoretical works stem from the concept of representing soil by discrete springs with the soil subgrade modulus as the spring constant. This approach was modified to account for plastic deformation of soil by incorporating nonlinearity in the soil springs (Matlock and Reese 1960; McClelland and Focht 1958). Further development of this method led to the well-known *p-y* method (Reese and Cox 1968; Matlock 1970; Reese et al. 1974, 1975). The continuum approach was also used for the analysis of laterally loaded piles. Poulos (1971a, b) applied an integral equation method of analysis while Banerjee and Davies (1978) used a similar boundary element algorithm. Sun (1994) and Basu et al. (2009) used variational principles to obtain analytical solutions for lateral pile displacements in elastic media. Guo and Lee (2001) assumed a stress field using the Fourier series and obtained a load transfer method for laterally loaded piles. These apart, the FEM (Desai and Appel 1976; Bhowmik and Long 1991; Bransby 1999; Hsiung and Chen 1997), finite elements coupled with Fourier series (Randolph 1981; Carter and Kulhawy 1992), the finite difference method (Klar and Frydman 2002; Ng and Zhang 2001), the boundary element method (Budhu and Davies 1988), and the upper-bound method of plasticity (Murff and Hamilton 1993) have been used to analyze laterally loaded piles.

In this paper, the FEM coupled with Fourier techniques is used to analyze laterally loaded piles embedded in elastic continua. Piles with different lengths, flexibilities, and boundary conditions are considered. Subsurface profiles with constant and linearly varying moduli are assumed. Additionally, a two-layer profile is considered. A parametric study is performed in which the important variables governing the pile behavior are identified. Based on the study, design equations are proposed using which pile deflection, slope, and bending moment can be calculated if the correct elastic soil modulus is available. Design examples are provided to illustrate the use of the analysis.

Analysis

Cylindrical piles with a lateral load F_a and moment M_a acting at the head are considered in this paper (Fig. 1). The pile is described by its radius r_p, length L_p, and Young's modulus E_p. The soil is described by its shear modulus G_s and Poisson's ratio υ_s. Three types of soil profiles are considered in this paper

1. Homogeneous soil in which G_s remains spatially constant;
2. Heterogeneous soil in which G_s increases linearly with depth from zero value at the ground surface; and
3. Two-layer soil with different values of G_s that remain spatially constant within each layer (Fig. 2).

[1]Former Graduate Student, Dept. of Civil and Environmental Engineering, Univ. of Connecticut, Storrs, CT 06269. E-mail: wthigginsiv@gmail.com

[2]Former Undergraduate Student, Dept. of Civil and Environmental Engineering, Univ. of Connecticut, Storrs, CT 06269. E-mail: celio.vasquez@uconn.edu

[3]Assistant Professor, Dept. of Civil and Environmental Engineering, Univ. of Waterloo, Waterloo, ON, Canada N2L 1W7 (corresponding author). E-mail: dipanjan.basu@uwaterloo.ca

[4]Professor of Civil Engineering, Division of Engineering, Colorado School of Mines, Golden, CO 80401. E-mail: d.v.griffiths@mines.edu

Note. This manuscript was submitted on March 22, 2011; approved on September 4, 2012; published online on September 5, 2012. Discussion period open until December 1, 2013; separate discussions must be submitted for individual papers. This paper is part of the ***Journal of Geotechnical and Geoenvironmental Engineering***, Vol. 139, No. 7, July 1, 2013. ©ASCE, ISSN 1090-0241/2013/7-1096–1103/$25.00.

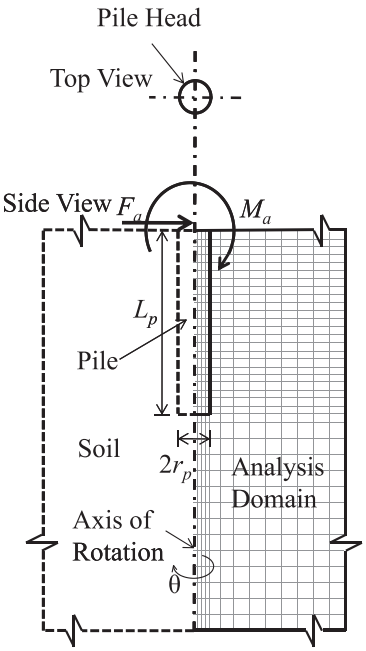

Fig. 1. Schematic of analysis domain: pile; applied load; FE mesh

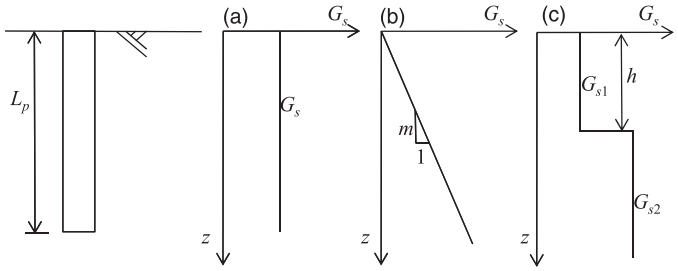

Fig. 2. Plots of soil shear modulus versus depth: (a) constant stiffness with depth; (b) stiffness linearly increasing with depth with zero value at the ground surface; (c) two-layer soil with constant stiffness in each layer

The Fourier finite-element (FE) code developed by Smith and Griffiths (2004), which calculates the response of axisymmetric solids subject to nonaxisymmetric loads, was used for the purpose of analysis. The domain of analysis is represented by a two-dimensional (2D) rectangular plane, which is an axisymmetric plane of the cylindrical problem geometry. The analysis domain was chosen sufficiently large so as to remove any boundary effects. The distance between the horizontal bottom boundary of the domain and the pile base was at least one pile length. The outer vertical boundary of the domain was maintained at a radial distance of at least 1.5 times the pile length from the pile-soil interface.

The analysis domain was discretized using rectangular, quadratic elements. Each element in the 2D plane represents an annulus centered on the axis of symmetry. The mesh density was different for different pile geometries. For the long piles, it was necessary to maintain a high mesh density near the pile head where the deformations are predominant. On the other hand, for short piles, a uniformly dense mesh was required throughout the entire pile length. The cases in which the stiffness varied with depth required more rows of elements so as to smoothly approximate the linear variation. About 10,000 elements were used in each mesh. Convergence tests were performed on all the meshes before final results were accepted. The accuracy of the analysis was ensured by comparing selected results with the results of equivalent three-dimensional (3D) FE analysis obtained using the software *ABAQUS*. The match of the pile deflection profiles between the present analysis and the 3D FE analysis was perfect (with the curves falling on top of each other).

In the analysis, the applied loads are defined using harmonic functions of the angle θ representing the angular distance out from the 2D plane in the tangential direction. For example, a node on the 2D plane loaded using the 0th harmonic represents a uniform load acting on the ring that the node represents. A node loaded using the first harmonic has a magnitude that varies sinusoidally with θ. The horizontal load and moment are created by applying horizontal and vertical loads, respectively, at the nodes representing the pile head using the first harmonic. Using the proper harmonic, the applied horizontal load was distributed along θ in such a way that its direction always coincided with the direction of the applied horizontal load. The vertical load was distributed along θ in such a way that it was upward on one-half of the pile-head section and downward on the other-half, thereby creating a moment at the head (Smith and Griffiths 2004).

Results

Modification of Soil Shear Modulus

Randolph (1981) found that the effect of soil Poisson's ratio υ_s on the response of laterally loaded piles was minimal, and can be adequately captured by using an equivalent shear modulus G_s^* of the elastic soil given by

$$G_s^* = G_s(1 + 0.75\upsilon_s) \tag{1}$$

where G_s = actual shear modulus of soil. The observation of Randolph (1981) was confirmed to be true by our analysis, and hence, G_s^* is used in our analysis to represent the elastic properties of soil. Consequently, for soils with stiffness increasing linearly with depth z, the gradient $m = dG_s/dz$ requires modification as

$$m^* = m(1 + 0.75\upsilon_s) = \frac{dG_s}{dz}(1 + 0.75\upsilon_s) \tag{2}$$

Effect of Relative Stiffness of Pile and Soil

The stiffness ratio E_p/G_s^* has a strong influence on the lateral pile response. For a pile of given geometry and modulus, the stiffness ratio governs whether it behaves as a flexible or a rigid pile. Figs. 3(a and b) show the normalized head deflection w of piles with free heads as a function of the relative stiffness E_p/G_s^* caused by applied force F_a and moment M_a, respectively, for different values of pile slenderness ratio L_p/r_p. The plots are generated for piles embedded in homogeneous soil profiles. For the range of E_p/G_s^* considered in this study, piles with a large slenderness ratio of 80 or greater behave as long flexible piles with the normalized head deflection decreasing continuously with increasing E_p/G_s^*. For piles with slenderness ratio less than 80, there is a divergence from the flexible behavior toward rigid behavior as E_p/G_s^* increases. The rigid behavior is characterized by no change in the normalized pile head deflection with increasing E_p/G_s^*. At large values of E_p/G_s^*, the pile does not bend like a flexible beam but undergoes rigid translation and rotation thereby making the effect of E_p on pile behavior negligible. Consequently, the behavior of rigid piles depends only on the pile

J. Geotech. Geoenviron. Eng., 2013, 139(7): 1096-1103

slenderness ratio (i.e., on the pile geometry). For a particular value of slenderness ratio, if the ratio E_p/G_s^* is greater than a threshold value, then the pile behaves as a rigid pile. This threshold value of E_p/G_s^* can be related to the pile slenderness ratio as

$$\left(\frac{E_p}{G_s^*}\right)_{\mathrm{RT}} = 44\left(\frac{L_p}{r_p}\right)^{3.23} \tag{3}$$

where the subscript RT = rigid threshold. The plots in Figs. 3(a and b) to the right of the threshold line [Eq. (3)] represent the behavior of rigid piles for which E_p/G_s^* is greater than $(E_p/G_s^*)_{\mathrm{RT}}$.

The behavior of flexible piles, on the other hand, depends on both the relative stiffness and the slenderness ratio. For long flexible piles, the length is so large that the pile-base conditions do not affect the behavior of the pile head. For such long and slender piles, the lateral behavior can be adequately expressed in terms of E_p/G_s^* alone. As shown in Figs. 3(a and b), the pile with $L_p/r_p \geq 80$ behaves like a long pile. The head deflection for such long piles can be expressed algebraically by fitting a curve through the long pile response plots shown in Figs. 3(a and b) as

$$w = 0.34\frac{F_a}{G_s^* r_p}\left(\frac{E_p}{G_s^*}\right)^{-0.18} + 0.30\frac{M_a}{G_s^* r_p^2}\left(\frac{E_p}{G_s^*}\right)^{-0.43} \tag{4}$$

Similarly, the head rotation (slope) of long flexible piles is independent of pile slenderness ratio and can be expressed as

$$\left(\frac{dw}{dz}\right)_{z=0} = 0.28\frac{F_a}{G_s^* r_p^2}\left(\frac{E_p}{G_s^*}\right)^{-0.43} + 0.90\frac{M_a}{G_s^* r_p^3}\left(\frac{E_p}{G_s^*}\right)^{-0.72} \tag{5}$$

The response of piles embedded in soil profiles in which the shear modulus increases linearly with depth from a zero value at the surface is similar to those observed for piles in homogeneous profiles described previously (Higgins and Basu 2011). For such linearly varying profiles, the relative stiffness of pile and soil is adequately represented by the ratio $E_p/m^* r_p$ (Randolph 1981). The threshold $(E_p/m^* r_p)_{\mathrm{RT}}$, exceeding which the piles behave as rigid piles, is given by

$$\left(\frac{E_p}{m^* r_p}\right)_{\mathrm{RT}} = 119\left(\frac{L_p}{r_p}\right)^{3.45} \tag{6}$$

The head deflection and slope of the long flexible piles, for which $(E_p/m^* r_p) < (E_p/m^* r_p)_{\mathrm{RT}}$, are given by the fitted equations

$$w = 0.55\frac{F_a}{m^* r_p^2}\left(\frac{E_p}{m^* r_p}\right)^{-0.33} + 0.53\frac{M_a}{m^* r_p^3}\left(\frac{E_p}{m^* r_p}\right)^{-0.54} \tag{7}$$

$$\left(\frac{dw}{dz}\right)_{z=0} = 0.50\frac{F_a}{m^* r_p^3}\left(\frac{E_p}{m^* r_p}\right)^{-0.54} + 1.23\frac{M_a}{m^* r_p^4}\left(\frac{E_p}{m^* r_p}\right)^{-0.78} \tag{8}$$

Pile heads are rarely free to translate and rotate as piles are most of the time attached to a structural element above. If a cap is present, the head rotation is significantly restrained and it is customary to assume that there is zero rotation at the head. The response of such fixed-head piles in homogeneous soil profiles are shown in Fig. 4. The general trend of the normalized head deflection versus stiffness ratio plots for fixed-head piles is similar to that observed for

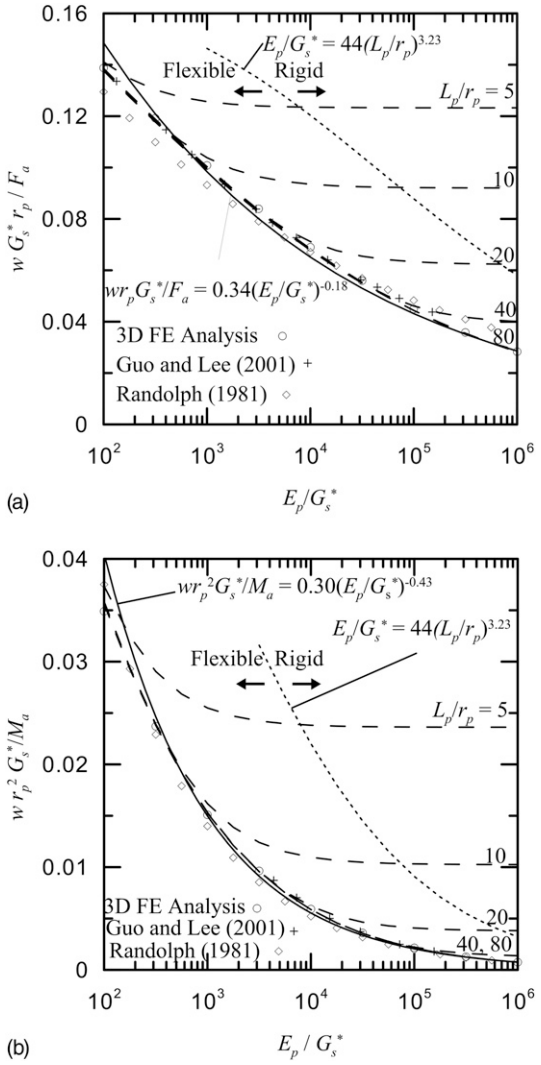

Fig. 3. Dimensionless pile head displacement versus stiffness ratio for free-head piles in homogeneous soil subjected to applied (a) lateral force; (b) moment at the head

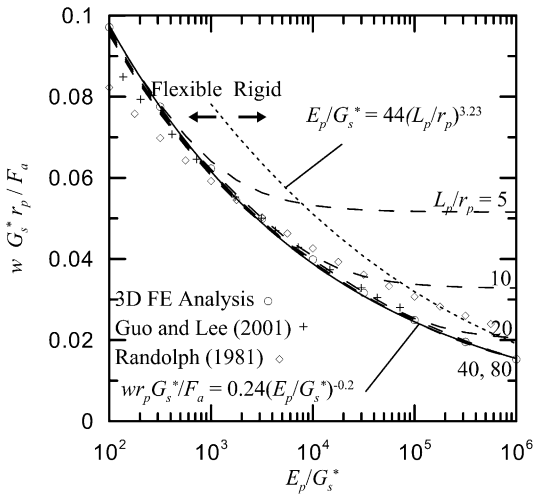

Fig. 4. Dimensionless pile head displacement versus stiffness ratio for fixed-head piles in homogeneous soil profiles subjected to applied lateral force at the head

J. Geotech. Geoenviron. Eng., 2013, 139(7): 1096-1103

the corresponding cases of free-head piles described previously (Higgins and Basu 2011).

The fixed-head piles with $(E_p/G_s^*) > (E_p/G_s^*)_{RT}$ undergo rigid translation from application of the applied force F_a, and do not exhibit any rigid rotation. Eqs. (3) and (6) describing $(E_p/G_s^*)_{RT}$ for free-head piles in homogeneous and linearly varying soil profiles, respectively, were found to be valid for the corresponding cases of fixed-head piles as well. The head deflection of long, flexible, fixed-head piles in homogeneous soil is obtained by fitting a curve to the plots corresponding to long piles in Fig. 4 as

$$w = 0.24\frac{F_a}{G_s^* r_p}\left(\frac{E_p}{G_s^*}\right)^{-0.20} \tag{9}$$

The fitted equation for the head deflection of fixed-head long piles in soil with linearly varying modulus [Fig. 2(b)] is obtained as

$$w = 0.31\frac{F_a}{m^* r_p}\left(\frac{E_p}{m^* r_p}\right)^{-0.35} \tag{10}$$

In addition to pile deflection, the bending moments at pile cross sections are important for the design of piles. When a moment is applied at a free pile head, the maximum bending moment M_{max} is equal to the applied moment and occurs at the pile head (Randolph 1981). The maximum bending moment from an applied horizontal force on free-head piles occurs at a finite depth below the ground surface. Fig. 5 shows the normalized maximum bending moment in free-head piles, from an applied horizontal force at the head, as a function of the relative stiffness in a homogeneous soil profile. For long flexible piles, M_{max} is independent of the pile slenderness ratio and can be expressed as (Randolph 1981)

$$M_{max} = 0.20F_a\, r_p\left(\frac{E_p}{G_s^*}\right)^{0.29} \tag{11}$$

Similarly, for long flexible piles in soil profiles in which the modulus increases linearly with depth from zero at the surface, M_{max} is given by

$$M_{max} = 0.40F_a\, r_p\left(\frac{E_p}{m^* r_p}\right)^{0.22} \tag{12}$$

For shorter piles, M_{max} depends on the pile slenderness ratio and, as the relative stiffness increases, M_{max} deviates from the trend followed by long piles. At large values of the stiffness ratio, M_{max} of shorter piles becomes independent of the stiffness ratio, indicating a rigid behavior.

Effect of Pile Slenderness Ratio

It is clear from the preceding discussion that the behavior of rigid piles and of flexible piles with moderately long lengths depends on pile slenderness ratio L_p/r_p. Thus, the effect of the slenderness ratio on pile behavior is investigated further. The normalized pile head deflection from applied force and moment are plotted as a function of L_p/r_p in Figs. 6(a and b), respectively, for different values of E_p/G_s^*. These plots are generated for free-head piles in homogeneous soil profiles. For the range of slenderness ratio considered in the study, a value of $E_p/G_s^* = 10^5$ or greater produced rigid piles. For piles with E_p/G_s^* less than 10^5, the pile response deviates from the

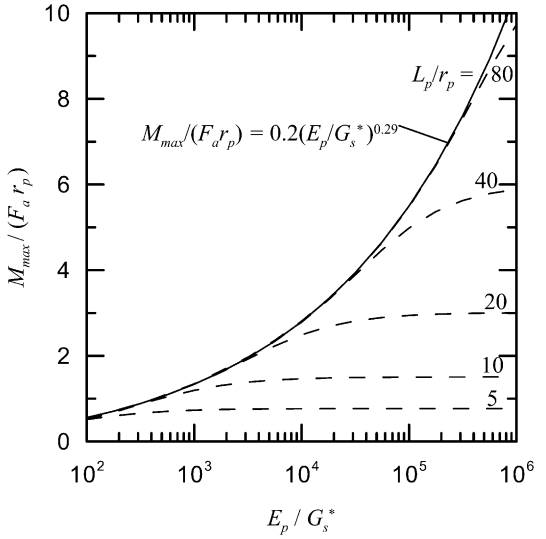

Fig. 5. Dimensionless maximum bending moment versus stiffness ratio for free-head piles in homogeneous soil and subjected to an applied horizontal force at the head

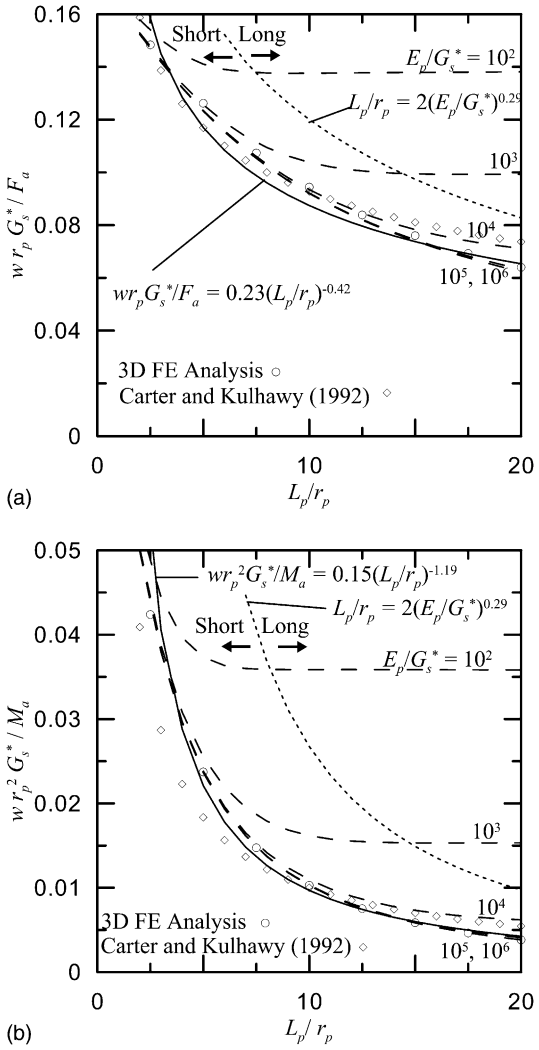

Fig. 6. Dimensionless pile head displacement versus slenderness ratio for free-head piles in homogeneous soil profiles subjected to (a) applied lateral force; (b) applied moment at the head

J. Geotech. Geoenviron. Eng., 2013, 139(7): 1096-1103

rigid behavior and there is a threshold value of L_p/r_p exceeding which the normalized head deflection becomes independent of the slenderness ratio implying that the behavior is that of flexible long piles. This threshold value of L_p/r_p represents the critical slenderness ratio $(L_p/r_p)_C$ and can be related to the stiffness ratio E_p/G_s^* as (Randolph 1981)

$$\left(\frac{L_p}{r_p}\right)_C = 2\left(\frac{E_p}{G_s^*}\right)^{0.29} \tag{13}$$

Piles with $(L_p/r_p) > (L_p/r_p)_C$ behave as long flexible piles and the length that produces the slenderness ratio equal to $(L_p/r_p)_C$ is often referred to as the critical length L_c of pile. L_c essentially represents a threshold length such that any additional pile length does not have any impact on the lateral pile response. Eq. (13) indicates that whether a pile behaves as a flexible long pile or not depends not only on its physical length but also on the relative stiffness E_p/G_s^*.

Because the behavior of rigid piles depends only on pile slenderness ratio, Figs. 6(a and b) can be used to obtain a fitted algebraic equation for pile head deflection of free-head, rigid piles in homogeneous soil as

$$w = 0.23\left(\frac{F_a}{G_s^* r_p}\right)\left(\frac{L_p}{r_p}\right)^{-0.42} + 0.15\left(\frac{M_a}{G_s^* r_p^2}\right)\left(\frac{L_p}{r_p}\right)^{-1.19} \tag{14}$$

The rotation of free-head, rigid piles in homogeneous soil can be similarly expressed as

$$\left(\frac{dw}{dz}\right)_{z=0} = 0.15\left(\frac{F_a}{G_s^* r_p^2}\right)\left(\frac{L_p}{r_p}\right)^{-1.19} + 0.21\left(\frac{M_a}{G_s^* r_p^3}\right)\left(\frac{L_p}{r_p}\right)^{-2.10} \tag{15}$$

The normalized head deflection versus slenderness ratio relationships for free-head piles in soil profiles with the shear modulus increasing linearly with depth from zero at the surface are similar to those obtained for homogeneous profiles. The critical slenderness ratio of free-head piles in linearly varying soil profiles can be obtained as (Randolph 1981)

$$\left(\frac{L_p}{r_p}\right)_C = 2\left(\frac{E_p}{m^* r_p}\right)^{0.22} \tag{16}$$

The head deflection and rotation of free-head rigid piles in linearly varying soil can be obtained as

$$w = 0.37\frac{F_a}{m^* r_p^2}\left(\frac{L_p}{r_p}\right)^{-1.14} + 0.29\frac{M_a}{m^* r_p^3}\left(\frac{L_p}{r_p}\right)^{-1.99} \tag{17}$$

$$\left(\frac{dw}{dz}\right)_{z=0} = 0.29\frac{F_a}{m^* r_p^3}\left(\frac{L_p}{r_p}\right)^{-1.99} + 0.33\frac{M_a}{m^* r_p^4}\left(\frac{L_p}{r_p}\right)^{-2.93} \tag{18}$$

The trends exhibited by the fixed-head piles are similar to those by the free-head piles (Higgins and Basu 2011). Thus, Eqs. (13) and (16) describing $(L_p/r_p)_C$ for free-head piles in homogeneous and linearly varying soil profiles, respectively, were found to be valid for the corresponding cases of fixed-head piles as well. The normalized head deflection for fixed-head piles in homogeneous soil as a function of pile slenderness ratio is plotted in Fig. 7. The fitted equation for head deflection (translation) of fixed-head rigid piles in homogeneous soil is obtained from Fig. 7 as

$$w = 0.14\left(\frac{F_a}{G_s^* r_p}\right)\left(\frac{L_p}{r_p}\right)^{-0.65} \tag{19}$$

The fitted equation for head deflection (translation) of fixed-head piles in linearly varying soil profile is obtained as

$$w = 0.14\frac{F_a}{m^* r_p^2}\left(\frac{L_p}{r_p}\right)^{-1.50} \tag{20}$$

Fig. 8 shows the normalized maximum bending moment in free-head piles in homogeneous soil, from an applied horizontal force at the head, as a function of the pile slenderness ratio. For rigid piles in

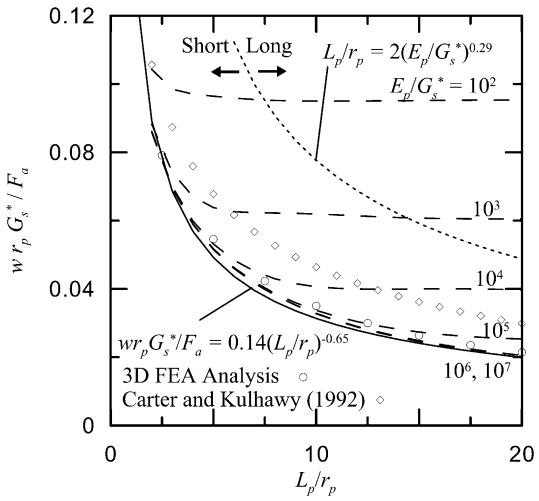

Fig. 7. Dimensionless pile head displacement versus slenderness ratio for fixed-head piles in homogeneous soil profiles subjected to applied lateral force at the head

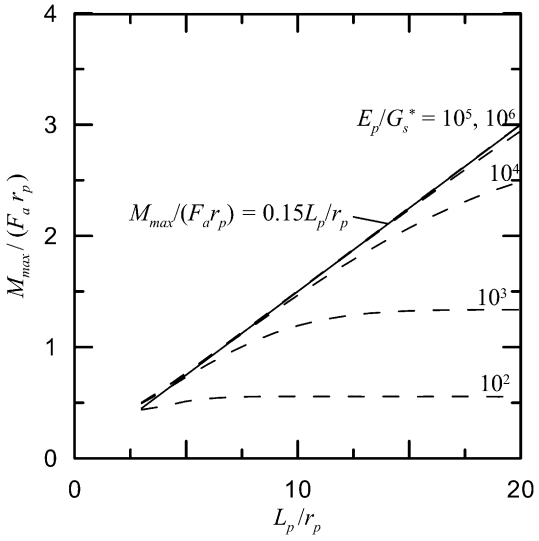

Fig. 8. Dimensionless maximum bending moment versus slenderness ratio for free-head piles in homogeneous soil and subjected to an applied horizontal force at the head

J. Geotech. Geoenviron. Eng., 2013, 139(7): 1096-1103

homogeneous soil with large values of relative stiffness, the maximum bending moment is given by

$$M_{\max} = 0.15F_a\, r_p \left(\frac{L_p}{r_p}\right) = 0.15F_a L_p \tag{21}$$

Similarly, $M_{\max}$ for rigid piles in linearly varying profiles is given by

$$M_{\max} = 0.27F_a\, r_p \left(\frac{L_p}{r_p}\right) = 0.27F_a L_p \tag{22}$$

The fitted equations of pile head deflection, rotation, and maximum bending moment given in the preceding equations are valid either for rigid piles or for flexible long piles. For flexible piles with intermediate length, no simple equation can be proposed as their behavior depends on both the pile slenderness ratio and relative pile-soil stiffness, and appropriate normalizations with respect to both these parameters are difficult to obtain. Thus, for these intermediate-sized piles, the head deflection, rotation, and maximum bending moment may be estimated from the plots given in Figs. 3–8 and in Higgins and Basu (2011).

Piles in Two-Layer Profiles

Often, soil profiles have discrete layers with distinct properties. For such profiles, the results obtained here are not strictly valid. Although an exhaustive study with different possible soil layering is beyond the scope of this paper, a simple case of two-layer profile is investigated here. The two-layer profile is characterized by the equivalent shear moduli G^*_{s1} and G^*_{s2} of the top (first) and the underlying (bottom) layers, respectively, and by the thickness h of the top layer [Fig. 2(c)]. The bottom layer is assumed to extend to great depth.

Fig. 9 shows the normalized head deflection of long, flexible free-head piles in two-layer soil profiles from applied lateral force at the head as a function of the relative stiffness E_p/G^*_{s1}. The deflections in these plots are normalized with respect to the shear modulus G^*_{s1} of the top layer, the thickness h of which is fixed at half the critical pile length L_c. The plots are generated for different values of soil stiffness ratio G^*_{s2}/G^*_{s1} with a fixed value of G^*_{s1}. Thus, for the case with $G^*_{s2}/G^*_{s1} = 0.5$, the bottom layer is made weaker than the top layer while, for the case with $G^*_{s2}/G^*_{s1} = 2.0$, the bottom layer is made twice as strong as the top layer. For a fixed value of stiffness of the top layer, a weaker bottom layer results in greater head deflection while a stronger bottom layer results in less head deflection than that of the corresponding homogeneous case. This difference in head deflection, however, decreases with increasing E_p/G^*_{s1}.

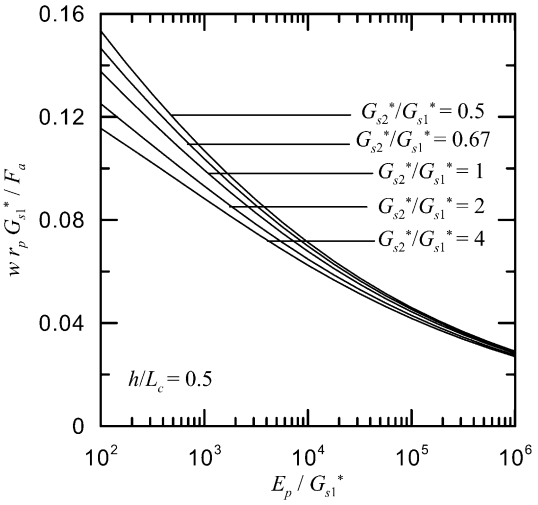

Fig. 9. Dimensionless pile head displacement versus relative stiffness for long, flexible free-head piles in two-layer soil from applied lateral force

Fig. 10 shows the effect of the thickness h of the top layer on the response of free-head long piles in two-layer soil. If the bottom layer is weak as in the case with $G^*_{s2}/G^*_{s1} = 0.5$, then a greater h/L_c produces less head deflection while the reverse is true for $G^*_{s2}/G^*_{s1} = 2.0$.

Based on Figs. 9 and 10, the head deflection of long, flexible free-head piles in two-layer soil profiles, from an applied horizontal force at the head, can be expressed as

$$w = k_1 \frac{F_a}{G^*_{s1}\, r_p} \left(\frac{E_p}{G^*_{s1}}\right)^{-k_2} \tag{23}$$

where the regression coefficients k_1 and k_2 are given in Table 1.

Figs. 11 and 12 show the response of rigid piles in two-layer soil. In these figures, the pile head deflection, normalized with respect to G^*_{s1}, is plotted as a function of pile slenderness ratio L_p/r_p. Fig. 11 shows that, for a fixed top layer with thickness $h = 0.5L_p$ and stiffness G^*_{s1}, the head deflection decreases with increasing G^*_{s2}/G^*_{s1}. Fig. 12 shows that, if the thickness of the top layer increases, then head deflection increases if the bottom layer is stronger than the top

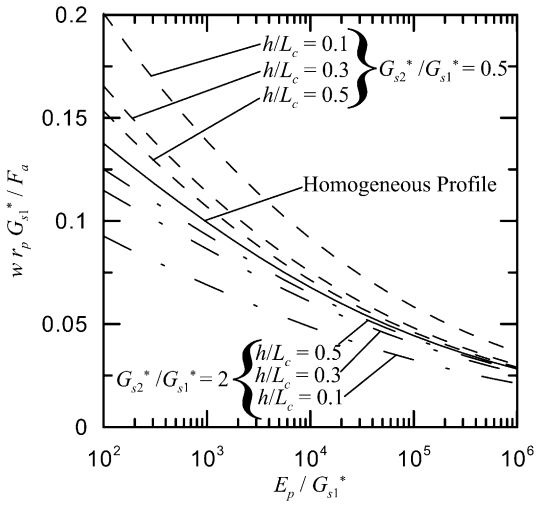

Fig. 10. Dimensionless pile head displacement versus relative stiffness for long, flexible free-head piles in two-layer soil from applied lateral force showing the effect of layer thickness

Table 1. Regression Coefficients for Head Deflection of Long, Flexible Free-Head Piles in Two-Layer Soil [Eq. (23)]

G^*_{s2}/G^*_{s1}	h/L_c	k_1	k_2
0.5	0.1	0.47	0.18
	0.3	0.38	0.18
	0.5	0.37	0.18
0.67	0.5	0.35	0.18
1.0 (homogeneous)	—	0.34	0.18
2.0	0.1	0.21	0.16
	0.3	0.26	0.16
	0.5	0.28	0.16
4.0	0.5	0.26	0.16

J. Geotech. Geoenviron. Eng., 2013, 139(7): 1096-1103

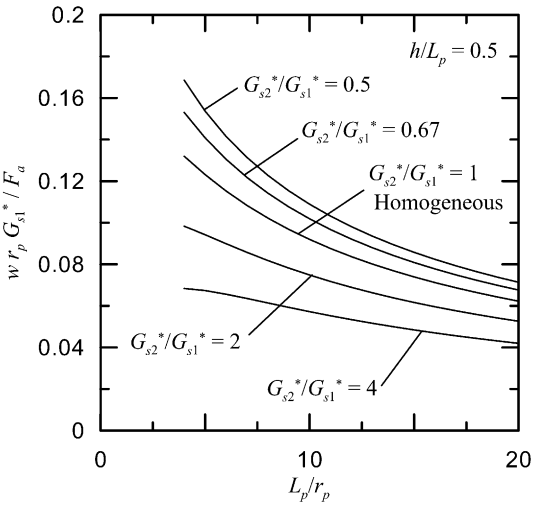

Fig. 11. Dimensionless pile head displacement versus slenderness ratio for rigid, free-head piles in two-layer soil from applied lateral force showing the effect of soil stiffness ratio

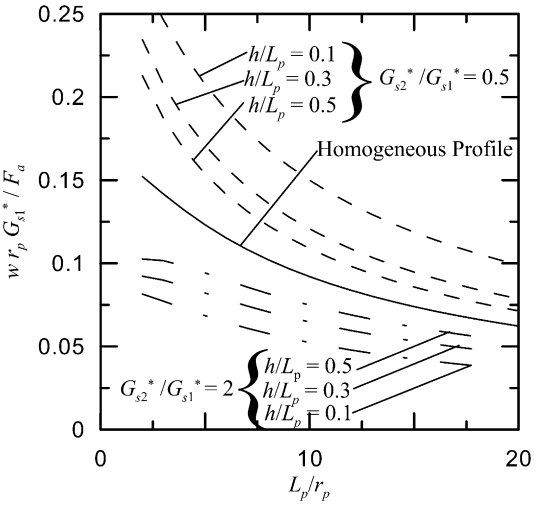

Fig. 12. Dimensionless displacement versus slenderness ratio for rigid, free-head piles in two-layer soil from applied lateral force showing the effect of layer thickness

layer, while the head deflection decreases as the thickness of the top layer increases if the bottom layer is weaker than the top layer. Using Figs. 11 and 12, the head deflection of rigid free-head piles in two-layer soil, from an applied horizontal force, can be obtained as

$$w = k_3\left(\frac{F_a}{G_{s1}^* r_p}\right)\left(\frac{L_p}{r_p}\right)^{-k_4} \tag{24}$$

where the regression coefficients k_3 and k_4 are given in Table 2.

Numerical Examples

Two design examples are considered in this section—one with constant modulus and the other with linearly varying modulus. In both the examples it is assumed that the piles are first designed against axial loads and then checked against tolerable lateral deflections. In addition, a case study of a lateral pile load test is analyzed.

Table 2. Regression Coefficients for Head Deflection of Rigid Free-Head Piles in Two-Layer Soil [Eq. (24)]

G_{s2}^*/G_{s1}^*	h/L_p	k_3	k_4
0.5	0.1	0.46	0.50
	0.3	0.37	0.50
	0.5	0.37	0.54
0.67	0.5	0.33	0.52
1.0 (homogeneous)	—	0.23	0.42
2.0	0.1	0.12	0.39
	0.3	0.14	0.36
	0.5	0.19	0.41
4.0	0.5	0.12	0.33

A single drilled shaft is to be designed in a homogeneous clay layer with undrained shear strength $s_u = 150$ kPa. From the design considerations against axial loads it was found that a pile length of 15 m and a diameter of 600 mm is adequate. A lateral load of 300 kN and moment of 100 kN/m act on the pile. It is necessary to restrict the head deflection to within 25 mm. Assuming undrained conditions, it is reasonable to choose clay Poisson's ratio $\upsilon_s = 0.45$. The Young's modulus E_s of clay can be estimated from the relationship $E_s = 500 s_u$ (Selvadurai 1979) as 75,000 kPa. Thus, for the soil profile in question, $G_s = 0.5E_s/(1+\upsilon_s) = 25{,}862$ kPa and $G_s^* = G_s(1+0.75\upsilon_s) = 34{,}590$ kPa. Because drilled shafts are made of lightly reinforced concrete, $E_p = 24\times10^6$ kPa is a reasonable assumption, which makes $E_p/G_s^* = 694$. The pile slenderness ratio $L_p/r_p = 50$. Because the rigid threshold $(E_p/G_s^*)_{RT} = 44\times50^{3.23} = 13{,}524{,}642$ is much greater than the E_p/G_s^* of the pile, it behaves as a flexible member. The critical slenderness ratio $(L_p/r_p)_C = 2\times69^{0.29} = 6.8$ is less than the actual pile slenderness ratio. Therefore, the drilled shaft behaves as a long pile. Consequently, Eq. (4) can be used to estimate the pile head deflection—the estimated head deflection is 3.6 mm. Thus, the estimated lateral head deflection is less than the tolerable deflection of 25 mm, which makes the design satisfactory.

As a second example, a driven concrete pile, attached to a cap, is to be designed in a sandy soil deposit. Considering axial capacity, the pile has the dimensions $L_p = 20$ m and $r_p = 0.2$ m. A lateral force of 500 kN acts at the pile head. The tolerable lateral head deflection is 25 mm. The soil profile consists of very loose deposit near the ground surface although the relative density increases gradually with depth. The increase in the relative density with depth can be assumed to be approximately linear and a relative density of 80% was observed at a depth of 30 m. For dense sands, the Young's modulus E_s can be conservatively assumed to be 75,000 kPa (Selvadurai 1979). Because the sand near the ground surface is very loose, the Young's modulus can be assumed to be zero at the surface. The Poisson's ratio υ_s of sand can be reasonably assumed to be 0.2 (Selvadurai 1979). This makes the shear modulus $G_s = 31{,}250$ kPa at a depth of 30 m and zero at the ground surface. Thus, the gradient $m = dG_s/dz$ of the linear variation of shear modulus is equal to 1,042 kPa/m and $m^* = m(1+0.75\upsilon_s) = 1{,}198$ kPa/m. Because driven concrete piles are heavily reinforced, $E_p = 25\times10^6$ kPa is a reasonable assumption. Thus, for this pile, $L_p/r_p = 100$, $E_p/m^* r_p = 104{,}340$, $(E_p/m^* r_p)_{RT} = 945{,}250{,}599$, and $(L_p/r_p)_C = 25.4$. Therefore, the pile falls under the category of long, flexible fixed-head piles. The lateral head deflection is calculated as 11.3 mm using Eq. (10). Because the estimated head deflection is less than the tolerable deflection of 25 mm, the design is acceptable.

Finally, a field example of a pile load test performed by McClelland and Focht (1958) is analyzed. The length (L_p) and radius (r_p) of the pile are 23 m and 0.305 m, respectively, and the

J. Geotech. Geoenviron. Eng., 2013, 139(7): 1096-1103

pile was embedded into a normally consolidated clay. The pile was acted upon by a lateral force $F_a = 267$ kN and a negative moment $M_a = -325$ kN/m at the head. Randolph (1981) backcalculated the pile modulus E_p as 68.42×10^6 kN/m^2 from the reported pile flexural rigidity. Randolph (1981) further suggested that the shear modulus profile for the soil deposit at the test site can be approximated as $G_s = 0.8 \times 10^3$kN/m^2 with $\upsilon_s = 0.3$. Thus, for this case study, $m = 0.8 \times 10^3$ kPa/m, which makes $m^* = m(1 + 0.75\upsilon_s) = 980$ kPa/m, $L_p/r_p = 75.4$, $E_p/m^* r_p = 228{,}906$, $(E_p/m^* r_p)_{\mathrm{RT}} = 356{,}843{,}758$, and $(L_p/r_p)_{\mathrm{C}} = 30.2$. Therefore, the pile behaves as a flexible long pile. The head deflection predicted from Eq. (7) is 19.5 mm, which is very close to the observed head deflection of 20.5 mm in the field.

Conclusions

Laterally loaded piles embedded in elastic soil are analyzed using the Fourier FE analysis. Homogeneous soil profiles in which the soil modulus remains spatially constant, heterogeneous profiles in which the modulus increases linearly with depth from zero value at the ground surface, and two-layer soil profiles with different soil moduli within each layer are considered in the analysis. The effects of relative stiffness of pile and soil, and of pile slenderness ratio on pile head deflection, rotation, and maximum bending moment were investigated.

Three distinct behavior regimes were identified from the results. The piles with relative pile-soil stiffness greater than a threshold value behaved as rigid members. For these piles, the response depends only on the pile slenderness ratio L_p/r_p. The normalized head deflection decreases with increasing slenderness ratio. The piles with relative stiffness less than the threshold value behaved as flexible piles. When the slenderness ratio of flexible piles is greater than the critical slenderness ratio, the piles behave as long piles. For the long flexible piles, the behavior depends only on the relative pile-soil stiffness. The head deflection decreases as the relative stiffness increases. The behavior of flexible piles with moderate lengths, for which the slenderness ratio is less than the critical slenderness ratio, is dependent on both the relative stiffness and slenderness ratio. For these moderate-length piles, the head deflection decreases with increasing relative stiffness and with increasing slenderness ratio.

For piles in two-layer soil, there is an effect on the pile response of the thickness of the top layer and of the stiffness ratio G^*_{s2}/G^*_{s1} of the two layers. Lateral pile displacement increases not only if the stiffness of the top layer decreases but also if the stiffness of the bottom layer decreases. For a weaker top layer, the pile displacement increases as the thickness of the top layer increases. However, the effect of the bottom layer is marginal if the thickness of the top layer is very large.

Based on this study, algebraic equations describing the pile head deflection, rotation, and bending moment were developed by fitting the results of the FE analyses. Subsequently, the use of the analysis and the developed equations in design is illustrated with the help of numerical examples.

Acknowledgments

The authors wish to acknowledge the support of NSF grant CMMI-0970122 and KGHM Cuprum, Wrocław, Poland through the Framework 7 EU project on "Industrial Risk Reduction." Harry F. Martindale IV helped with plotting the figures, for which the authors are grateful.

References

Banerjee, P. K., and Davies, T. G. (1978). "The behavior of axially and laterally loaded single piles embedded in nonhomogeneous soils." *Geotechnique*, 28(3), 309–326.

Basu, D., Salgado, R., and Prezzi, M. (2009). "A continuum-based model for analysis of laterally loaded piles in layered soils." *Geotechnique*, 59(2), 127–140.

Bhowmik, S., and Long, J. H. (1991). "An analytical investigation of the behavior of laterally loaded piles." *Proc., Geotechnical Engineering Congress,* ASCE, Reston, VA, 2(27), 1307–1318.

Bransby, M. F. (1999). "Selection of *p-y* curves for the design of single laterally loaded piles." *Int. J. Numer. Anal. Methods Geomech.*, 23(15), 1909–1926.

Budhu, M., and Davies, T. G. (1988). "Analysis of laterally loaded piles in soft clays." *J. Geotech. Engrg.*, 114(1), 21–39.

Carter, J. P., and Kulhawy, F. H. (1992). "Analysis of laterally loaded shafts in rock." *J. Geotech. Engrg.*, 118(6), 839–855.

Desai, C. S., and Appel, G. C. (1976). "3-D analysis of laterally loaded structures." *Proc., 2nd Int. Conf. on Numerical Methods in Geomechanics*, Engineering Foundation Conferences, Blacksburg, VA, 405–418.

Guo, W. D., and Lee, F. H. (2001). "Load transfer approach for laterally loaded piles." *Int. J. Numer. Anal. Methods Geomech.*, 25(11), 1101–1129.

Higgins, W., and Basu, D. (2011). "Fourier finite element analysis of laterally loaded piles in elastic media." *Internal Geotechnical Rep. 2011-1*, Univ. of Connecticut, Storrs, CT.

Hsiung, Y., and Chen, Y. (1997). "Simplified method for analyzing laterally loaded single piles in clays." *J. Geotech. Geoenviron. Eng.*, 123(11), 1018–1028.

Klar, A., and Frydman, S. (2002). "Three-dimensional analysis of lateral pile response using two-dimensional explicit numerical scheme." *J. Geotech. Geoenviron. Eng.*, 128(9), 775–784.

Matlock, H. (1970). "Correlations for design of laterally loaded piles in soft clay." *Proc., 2nd Offshore Technology Conf.*, American Institute of Mining, Metallurgical, and Petroleum Engineers Inc., Englewood, CO, 577–594.

Matlock, H., and Reese, L. C. (1960). "Generalized solutions for laterally loaded piles." *J. Soil Mech. Found. Div.*, 86(5), 63–91.

McClelland, B., and Focht, J. A., Jr. (1958). "Soil modulus for laterally loaded piles." *Trans. ASCE*, ASCE, Reston, VA, 1049–1063.

Murff, J. D., and Hamilton, J. M. (1993). "P-Ultimate for undrained analysis of laterally loaded piles." *J. Geotech. Engrg.*, 119(1), 91–107.

Ng, C. W. W., and Zhang, L. M. (2001). "Three-dimensional analysis of performance of laterally loaded sleeved piles in sloping ground." *J. Geotech. Geoenviron. Eng.*, 127(6), 499–509.

Poulos, H. G. (1971a). "Behavior of laterally loaded piles: I. Single piles." *J. Soil Mech. Found. Div.*, 97(SM5), 711–731.

Poulos, H. G. (1971b). "Behavior of laterally loaded piles: III. Socketed piles." *J. Soil Mech. Found. Div.*, 98(SM4), 341–360.

Randolph, M. F. (1981). "The response of flexible piles to lateral loading." *Geotechnique*, 31(2), 247–259.

Reese, L., and Cox, W. (1968). "Soil behavior from analysis of tests of uninstrumented piles under lateral loading." *Proc., 72nd Annual Meeting,* ASTM, San Francisco, 161–176.

Reese, L. C., Cox, W. R., and Koop, F. D. (1974). "Analysis of laterally loaded piles in sand." *Proc., 6th Offshore Technol. Conf.*, American Institute of Mining, Metallurgical, and Petroleum Engineers Inc., Englewood, CO, 473–483.

Reese, L. C., Cox, W. R., and Koop, F. D. (1975). "Field testing and analysis of laterally loaded piles in stiff clay." *Proc., 7th Offshore Technol. Conf.*, American Institute of Mining, Metallurgical, and Petroleum Engineers Inc., Englewood, CO, 671–690.

Selvadurai, A. P. S. (1979). *Elastic analysis of soil-foundation interaction*, Elsevier, New York.

Smith, I. M., and Griffiths, D. V. (2004). *Programming the finite element method*, 4th Ed., Wiley, West Sussex, U.K.

Sun, K. (1994). "Laterally loaded piles in elastic media." *J. Geotech. Engrg.*, 120(8), 1324–1344.